EVALUATION OF A SLAM-BASED POINT CLOUD FOR DEFLECTION ANALYSIS IN HISTORIC TIMBER FLOORS

L.J. Sánchez-Aparicio [1,2], P. Villanueva-Llauradó [3], P. Sanz-Honrado [1], J.R. Aira-Zunzunegui [1], J. Pinilla Melo [1], D. González-Aguilera [2], D.V. Oliveira [4]

[1] Dept. of Architectural Construction and Technology, Escuela Técnica Superior de Arquitectura, Universidad Politécnica de Madrid, Avda. Juan de Herrera, 4, 28040 Madrid, Spain - lj.sanchez@upm.es; p.sanzh@alumnos.upm.es, (joseramon.aira, javier.pinilla) @upm.es

[2] Dept. of Cartographic and Land Engineering, University of Salamanca, Higher Polytechnic School of Ávila, Hornos Caleros, Ávila, Spain - (luisj, daguilera) @usal.es

[3] Dept. of Building Structures and Physics, Escuela Técnica Superior de Arquitectura, Universidad Politécnica de Madrid, Avda. Juan de Herrera, 4, 28040 Madrid, Spain - (paula.villanueva@upm.es)

[4] Dept. of Civil Engineering, ISISE, Campus de Azurém, Guimarães, Portugal - (danvco@civil.uminho.pt)

KEY WORDS: Wearable Mobile Mapping, Diagnostics, Timber floor, Simultaneous Location and Mapping, Deep Learning, Noise reduction

ABSTRACT:

This paper aims at evaluating the possibility of using wearable mobile mapping solutions as a tool for detecting deflections in timber floors. These construction systems are prone to present this type of damage due to the mechanical properties of the wood (relatively low flexural stiffness and creep behaviour). During this study we have evaluated the chance of introducing an additional stage to the general workflow. This stage is devoted to reduce the noise of the 3D point cloud by using the Statistical Outlier Removal filter in combination with a noise-reduction filter such as the Anisotropic filter, the PointCleannet or the Scored-based denoised networks (Deep Learning methods). According with our results, the use of this strategies improves the quality of the 3D point cloud form a qualitative and quantitative point of view. However, these improvements seem to be not sufficient for using this product as a universal source of information for deflection analysis. In this sense, and according with the sensor and study case exploited, this type of point clouds could be used in floors with 5-8-meter length and a relative deflection of about L/200 or higher.

1. INTRODUCTION

The guidelines for the conservation of cultural heritage buildings, codified in the Krakow Charter, underline the importance of studying the construction from a multidisciplinary and scientific point of view. Within this complex context, 3D point clouds are placed as a valuable source of information since they are able to represent the construction with great accuracy and resolution. Thanks to this, there are plenty of applications that use this product for different purposes that includes the diagnosis of the building (i.e. analysis of deformations, presence of moisture or generation of HBIM models among others) (Yang et al., 2022).

The acquisition of this valuable information could be carried out by using the laser scanning or the structure from motion photogrammetry. Concerning the first one, we can highlight the emergence of the Mobile LiDAR Systems. This type of laser scanner is able to generate 3D point clouds in movement, reducing data collection phase. Within this group, Wearable Mobile Mapping Systems (also named as Portable Mobile Mapping Systems) have been placed in a key position. This type of sensors are characterized by its reduced size and weight, being possible to equip them in backs (Nocerino et al., 2019). Thanks to this, it is possible to reduce data acquisition times in about 10 times (Di Filippo et al., 2018). However the final result, the 3D point cloud, is strongly affected by the data acquisition protocol as well as the processing parameters (Camiña et al., 2022; Di Filippo et al., 2018). Considering this, there are different works that deal with the accuracy assessment of this sensor, showing values near the centimetre (Camiña et al., 2022; Di Filippo et al., 2018; Nocerino et al., 2017; Rodríguez-Martín et al., 2018; Sánchez-Aparicio et al., 2019). These results place this sensor as a powerful digitalization tool for the creation of planimetric products (i.e. plans and sections) (Di Filippo et al., 2018). Nevertheless, there is not studies that deal with the analysis of this data for technical inspection in historic buildings (i.e. evaluation of deformations)

Under the basis previously exposed, this work aims at evaluating the advantages of integrating noise-reduction filters within the processing of WMMS point clouds. The goal of this application is to evaluate the possibility of integrating this type of sensor, which offers great advantages, into inspection tasks on which the accuracy is relevant (i.e. the evaluation of deflection in timber floors). To this end the article applies different filters that includes Deep Learning methods. The improvement of these filter is evaluated not only by calculating the statistical indexes (i.e. mean and standard deviation) but also by including an uncertainty analysis and a cross-validation for which a real study case is used.

2. MATERIALS AND METHODS

As it was stated previously, the aim of this work is to evaluate the capability of the novel WMMS sensors for evaluating the deflection in timber floors. According to this, it is necessary not only to capture the data of the timber floors by using this sensor, but also to contrast it with respect to a high-accuracy sensor such as a Terrestrial Laser Scanner.

Within this context the methodology used in this study comprised a total of three stages: i) the data acquisition; and ii) the data processing; and iii) the uncertainty propagation.

2.1 Data acquisition

The equipment chosen to perform this study included the used of the following LiDAR sensors: i) a Wearable Mobile Mapping

System (WMMS); and ii) a Terrestrial Laser Scanner (TLS). The first one was chosen due to its portability and performance (10 times higher than the static one) (Di Filippo et al., 2018). Meanwhile the second one was selected due to its accuracy.

2.1.1 Wearable Mobile Mapping System: The WMMS was the Zeb-Revo mobile mapping system (https://geoslam.com/). This device integrates a 2D rotating laser scanner head (Hokuyo UTM-30LX-F) rigidly coupled to an Inertial Measurement Unit (IMU) on a rotary engine. The data captured is stored in a small datalogger equipped within a backpack, being extremely portable (4.10 kg) and suitable for indoor spaces. This system is able to capture 40,000 points per second with a nominal accuracy of 1-3 cm and a range that varies from 0.60 to 30 m indoor and 0.60 to 15m outdoors. The autonomy of the equipment is about 4 hours.

After the data acquisition it was necessary to convert the 2D point cloud captured by the Hokuyo laser scanner and the data captured by the IMU. To this end it is necessary to apply the well-known Simultaneous Location and Mapping (SLAM) algorithm. This approach address with the problem of solving the position of a mobile system (such as the WMMS) inside an unknow environment, obtaining the 3D point cloud of the site. More specifically we use the full SLAM algorithm due to its accuracy, being carried out off-line. This approach has an incremental and iterative nature that allow to register the segment (2D point clouds) captured by the Hokuyo head one-by-one with the use of the IMU data. For more details about this strategy reader refers to di Fillipo et al. (Di Filippo et al., 2018).

2.1.2 Terrestrial Laser Scanner: In order to evaluate the performance of the WMMS in terms of accuracy, a high-precision laser scanner was used. More specifically the TLS Faro Focus 3D. This LiDAR sensor is based on the Amplitude Modulated Continuous Wave (AMCW) measure principle, highlighting by its data acquisition rate and accuracy. More specifically, this sensor is able to capture from 120,000 to 976,000 points per second with a nominal accuracy of 2 mm.

2.2 Data processing

The 3D point clouds obtained by both sensors were processed as follows: i) segmentation of the region of interest; ii) reduction of noise on the WMMS point cloud; iii) accuracy assessment of the resulting point clouds by using as error metric the discrepancy between the WMMS point clouds and the TLS one; and iv) uncertainty propagation.

All these stages were performed by using the open-source software CloudCompare® (https://www.danielgm.net/cc/) as well as several scripts programmed in Matlab® with the help of the uncertainty propagation library Uqlab (Marelli and Sudret, 2014).

The following sections will explain in detail all stages at exception of the first one since is considered a common step.

2.2.1 Noise reduction on the WMMS point cloud: Point cloud acquired from scanning sensors are perturbed by noise that could affect negatively in the subsequent products. In the case of the SLAM-based solutions, such as the WMMS sensors, the noise could be relevant, affecting negatively to the final product (i.e. extraction of sections or measures) (Sánchez-Aparicio et al., 2021). Thus, it is important not only to evaluate the discrepancies between the WMMS point clouds and the TLS one (which acts as reference data) (Di Filippo et al., 2018; Nocerino et al., 2017; Sánchez-Aparicio et al., 2019), but also to integrate additional noise-reduction strategies that allow to improve this aspect.

Under this basis we introduce an additional step in the point cloud processing which is the noise-reduction. During this stage we have evaluated different strategies that could allow us to reduce the intrinsic noise of this system. More specifically, we have tested the following state-of-art strategies:

- The Statistical Outlier Removal filter (SOR) (Rusu and Cousins, 2011): this method is a outlier removal strategy. In this context the outliers of a point cloud are all those points than are placed in areas on which the density of the data is lower than a threshold value. To this end the algorithm computes the mean distance between points of the 3D point cloud. During this step the algorithm computes the mean distance by using the *k*-nearest neighbours. Then, the algorithm extracts the mean and standard deviation of the population. Finally, the threshold value is computed as n*standard deviation. Where n is an input value defined by the user. Due to its nature, this strategy is evaluated in combination with the rest of the algorithms.
- The anisotropic algorithm (ANI) (Xu and Foi, 2019): this denoising strategy is based on aggregation of multiple polynomial surfaces computed on directional neighbourhoods. These neighbourhoods are locally adapted in accordance with the shape of the point cloud. This method is able to preserve fine features as well as sharp edges. It is worth mentioning that this algorithm was tested on another study case that used the same WMMS sensor (Sánchez-Aparicio et al., 2021), improving the original data.
- The PointCleanNet algorithm (PCN) (Rakotosaona et al., 2020): PCN algorithm is the pioneer of the Deep-Learning based denoising methods (Luo and Hu, 2021). This strategy employs a variant of the well-known PointNet (Qi et al., 2017). PointNet is a neural network that consumes point clouds, allowing to detect object or even to segment scenes (Qi et al., 2017). In the context of the noise-reduction, Rakotosaona et al. (2020) adapts this Network. Firstly, the network classifies and discards outliers, and then estimates the correction vectors that allow to project the noisy points on to the original clean surfaces. This approach is efficient against different noise and outliers levels (Rakotosaona et al., 2020).
- The Score-based denoising point cloud algorithm (SBD) (Luo and Hu, 2021): this algorithm is also based on a Deep-Learning strategy. In this case the denoise stage was performed by using a gradient ascent guided method which uses a log-density function. According with the authors, this method minimizes artefacts such as shrinkage and outliers, obtaining better results than the previous one.

2.2.2 Evaluation of the WMMS accuracy: This stage has the aim of evaluating the discrepancies between the 3D point cloud obtained in the previous stage (with noise reduction and without noise reduction) and 3D point cloud of the TLS. To this end the following methodology was applied: i) registration of each WMMS point cloud in the TLS coordinate system; ii) estimation of the discrepancies between the TLS and the WMMS; and iii) computation of the statistical indexes.

Firstly, each one of the WMMS point clouds were registered with the TLS point cloud with the aim of having all the data in the same coordinate system. To this end we used the Iterative Closets Points (ICP) algorithm (Besl and McKay, 1992). The ICP iteratively solves a minimization problem that allow to estimate the best transformation matrix between the moving point cloud (WMMS) and the fixed one (TLS).

Then, the discrepancies between each WMMS point cloud and the reference one was evaluated. These values were obtained by computing the cloud-to-cloud distance between point clouds. More specifically, we propose the use of the Multiscale Model to Model Cloud Comparison (M2C2) (Lague et al., 2013). This algorithm outperforms other cloud-to-cloud distance methods (Girardeau-Montaut et al., 2005), showing great robustness with respect to changes in point density and point cloud noise. Additionally, this algorithm is able to compute the signed distance thanks to the use of the normal vector of each point.
The results of this algorithms are used to compute the statistical indexes in accordance with the normality -or not- of the population (Rodríguez-Gonzálvez et al., 2017).

2.2.3 Uncertainty propagation: In statistics, the uncertainty propagation is the effect of the variable´s uncertainties (or measure errors) in the final output (model). This question has become a relevant topic nowadays in different fields of the applied sciences and engineering since it allows to simulate a model from a probabilistic point of view (Marelli and Sudret, 2014). This approach could be extended to 3D point clouds. In this sense the noise could be considered as an uncertainty source that could affect further studies (i.e. computation of measures). In the context of this study, the uncertainty propagation will refer to the effect of the discrepancies in the calculation of the relative deflection of timber floors. This parameter, the relative deflection, could be understood as the ratio between the length of the beam and its deflection.
The analysis of this effect was performed by using the Monte-Carlo method. This method is a sampling-based approach that is widely used for quantification and propagation of uncertainties (Zhang, 2021). In the Monte Carlo approach, the model is simulated *n* times by choosing a random sample of inputs that takes into consideration its Probabilistic Distribution Function (PDFs). This function could be obtained by using a curve fit method over the discrepancy map. Since the candidate functions could be Normal, Log-Normal, Weibull or Gamma among other, it is highlight recommended to perform a goodness-of-fit test (i.e. QQ-plots or the Shapiro-Wilk test) to choose the proper one (Garcia-Martin et al., 2020).

3. EXPERIMENTAL RESULTS

3.1 Study case

The case study is Nuestra Señora de Gracia Convent in Avila (Spain). This building was built with masonry bearing walls and unidirectional timber floors. The most antique parts include the roof timber trusses, part of the church in stone vaults, and a basement corridor comprising vaulted brick galleries. This inner space shows great complexity, lack of illumination and a large extension, being the WMMS the most effective solution in this sense.
Under this basis it was carried out the 3D digitalization of the space by using the Zeb-Revo laser scanner. The resulting 3D point cloud was made up by 143,637,353 points, speeding a total of 188 mins (this value includes the data acquisition and data processing) (Figure 1).

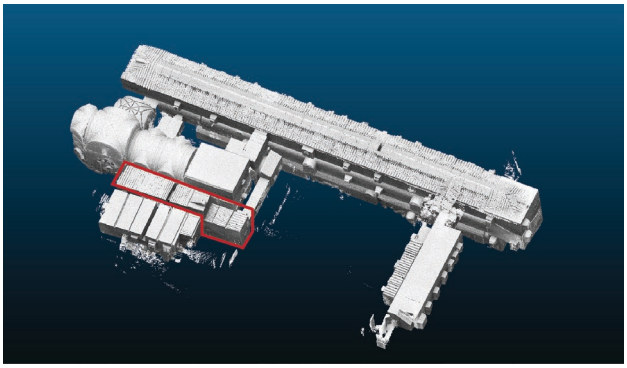

Figure 1. General view of the 3D point cloud

The interest of the case study lies in the diverse degree of deterioration of the timber floors (with presence of large deformations). Thus, it is required to perform a study current geometrical status of each beam element in order to design the most proper restoration strategy. This question demands the use of the 3D point clouds as a source of metric information for studying different parameters of structural interest such as:

- The span length: as the distance between the supports of the beam.
- The maximum deflection: understood as the distance between the point with largest deformation and the point with the less deformation

According to this, it was decided to make an in-depth evaluation of the most affected floors with the aim of evaluating the degree of uncertainty if we decide to use the 3D data provided by the WMMS point cloud. These floors were digitalized by the TLS Faro Focus 120 (Figure 2) in order to have a ground truth for comparison. For more details about the data acquisition and processing, reader must refer to Villanueva-Llauradó et al. (Villanueva Llauradó et al., 2022).

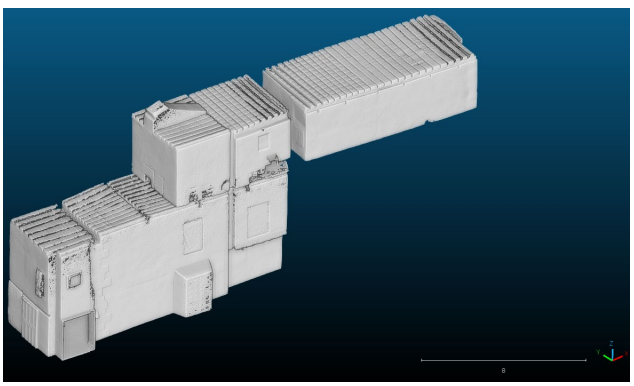

Figure 2. Detailed view of the floors used during this study

3.2 Noise reduction

Both 3D point clouds, WMMS and TLS, were registered in the same coordinate system by using the ICP algorithm. Thank to this it was possible to clean the non-overlapped areas with great efficiency since these areas will introduce noise in the discrepancy analysis.
Then we applied on the WMMS point cloud the filters highlighted in Section 2.2. In order to make as applicable as possible this process, we run all the algorithms with the default parameters, at exception of the SOR filter. In this case we studied different combination of parameters in order to mitigate the edge effects without removing points from other areas of

interest (Figure 3). This effect appears commonly in floors due to the geometrical disposition of the beams.
More specifically we tested the following combination of parameters:

- Number of points to compute the mean distance (*k*): we tested with 250,200,150,100,50,25,5.
- Standard deviation multiplier (*n*): 3.

a)

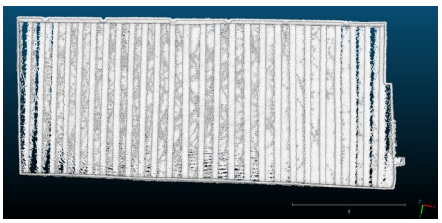

b)

Figure 3. Effects of the SOR filter over the default 3D point cloud: a) with a *k* of 250 and a *n* value of 3; and b) with a *k* of 10 and a *n* value of 3

The best results were obtained by considering a *k* value of 10. Lower values of *k* trend to remove relevant parts. Meanwhile higher values do not remove the outliers effectively.

3.3 Discrepancies between point clouds

The analysis of the discrepancies between each set of point clouds were carried out by using the M3C2 algorithm defined in Section 2.3. During this stage a total of two parameters were taken into consideration, namely: i) normal scale; and ii) projection scale. The first one allows us to define the diameter of the sphere used for computed the normal of each point. This value was fixed as 25 times the average surface roughness of the TLS point cloud as propose Lague et al. (Lague et al., 2013). Meanwhile, the second is used for defining the diameter of the cylinder used for searching the homologous point in the other 3d point cloud, allowing to reduce the computational time. This value was fixed in a point on which the resulting cylinder is able to capture at least 20 points in the TLS/WMMS point cloud (Lague et al., 2013).

a)

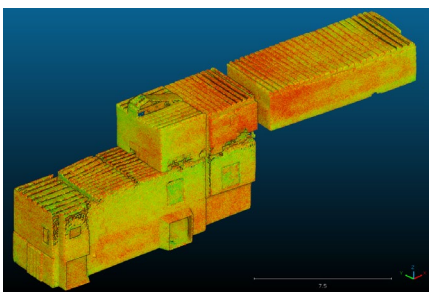

b)

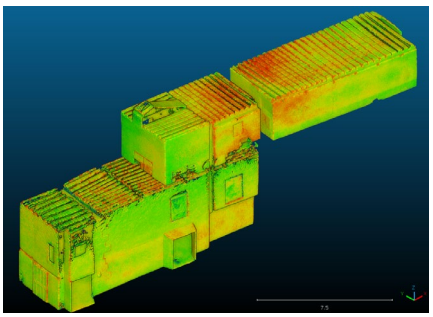

Figure 4. Map of discrepancies between the WMMS and TLS point clouds: a) before applying a noise reduction strategy; and b) after applying the strategy SBD + SOR. Red areas indicate discrepancies of 2.00 cm, green areas indicate quasi-null discrepancies

As a result, it was possible to obtain a full map of discrepancies (signed distances) between the WMMS and TLS point clouds (Figure 4).
The information contained in these maps was used for performing a qualitative and quantitative analysis of each resulting 3D point cloud.

3.3.1 Qualitative analysis of the 3D point cloud: The qualitative evaluation of the 3D point clouds was carried out by extracting several sections along the main axis of the timber floor. Then this information was visually checked, observing the performance of each strategy (Figure 5 and Figure 6).

a)

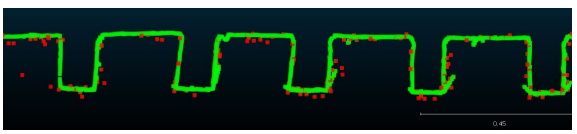

b)

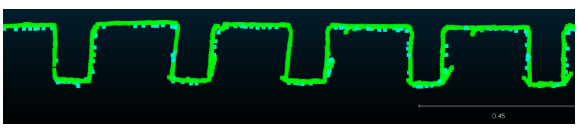

Figure 5. Transversal section of one beam: a) before noise reduction (red data); and b) after the application of the SBD + SOR strategy (cyan data). In green the data captured by the TLS

In general terms the application of the ANI and SBD algorithms (with and without SOR filter) improves the visual aspect of the point cloud (Figure 5 and Figure 6), making less disperse. However, the use of the PCN algorithm does not offer the same visual performance. After its application it was possible to observe some shrinkage problems. These problems were more prominent after the recurrent application of the Network (**Figure 7**).

a)

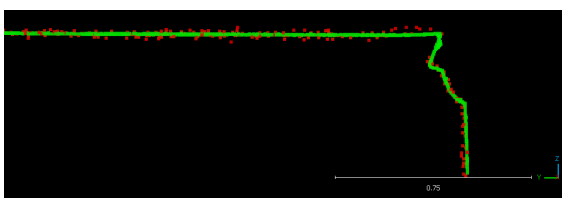

b)

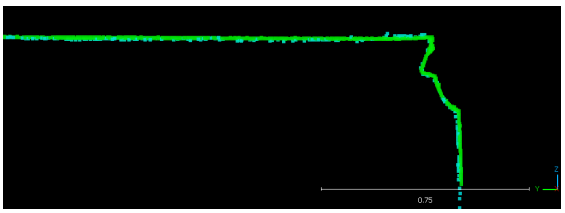

Figure 6. Longitudinal section of one beam: a) before noise reduction (red data); and b) after the application of the SBD + SOR strategy (cyan data). In green the data captured by the TLS

a)

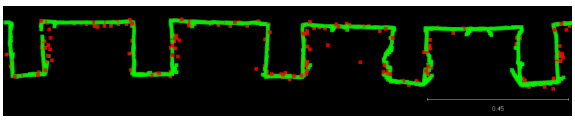

b)

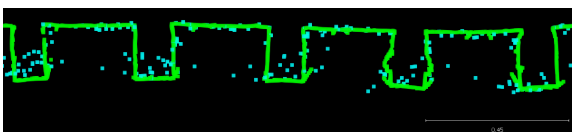

Figure 7. Results obtained after the application of the PCN algorithm: a) at the first iteration; and b) after applying the algorithm 10 times.

3.3.2 Quantitative analysis: accuracy assessment: Complementary to the qualitative analysis we decided to perform a quantitative evaluation. This stage allows us to have a deeper image about the performance of the different strategies by using statistical indexes as it was described in Section 2.3.
Firstly, we perform a normality test by using the QQ-plots as well as the Shapiro-Wilk test. In all the cases the population shows a normal distribution. Thus, it was required the use of parametric indexes in order to study each noise-reduction proposal. In this context the indices used where the mean (*m*) and the standard deviation (*stdev*). These indexes were supplemented with the interpercentile range (*IPR*) at 50% and 95% of confidence level. All these results are showed in the following table.
It is worth mentioning that all the combinations show a bias error (mean value). This error could be attributed to the SLAM processing since the floors evaluated are placed at different levels. So, we decided to study each floor separately, registering each one with respect to the TLS floor. After the application of this stage, the bias error disappeared, throwing the following results (Table 2 and Table 3).

WMMS point cloud	mean	stdev	IPR	
NO FILTER	0.003	0.007	0.010	0.027
NO FILTER + SOR	0.003	0.006	0.009	0.027
ANI	0.004	0.004	0.006	0.020
ANI + SOR	0.003	0.003	0.005	0.019
PCN (1 iter)	0.003	0.007	0.011	0.026
PCN + SOR (1 iter)	0.003	0.006	0.009	0.025
SBD	0.004	0.004	0.006	0.022
SBD + SOR	0.003	0.003	0.005	0.020

Table 1. Results obtained during the evaluation of the discrepancies between the different WMMS point clouds with respect to the TLS one

WMMS point cloud	mean	stdev	IPR	
NO FILTER	0.001	0.007	0.008	0.023
NO FILTER + SOR	0.001	0.006	0.008	0.021
ANI	0.001	0.004	0.005	0.019
ANI + SOR	0.001	0.004	0.005	0.017
PCN (1 iter)	0.001	0.007	0.009	0.023
PCN + SOR (1 iter)	0.001	0.007	0.009	0.024
SBD	0.001	0.004	0.006	0.022
SBD + SOR	0.000	0.003	0.005	0.020

Table 2. Results obtained for the upper floor.

WMMS point cloud	mean	stdev	IPR	
NO FILTER	0.001	0.007	0.008	0.022
NO FILTER + SOR	0.001	0.007	0.008	0.022
ANI	0.001	0.005	0.006	0.018
ANI + SOR	0.000	0.004	0.005	0.016
PCN (1 iter)	0.001	0.007	0.009	0.023
PCN + SOR (1 iter)	0.000	0.007	0.008	0.023
SBD	0.001	0.004	0.006	0.014
SBD + SOR	0.000	0.003	0.005	0.013

Table 3. Results obtained for the lower floor

3.3.3 Discussion of the results obtained during the accuracy assessment: All the data generated during the qualitative and quantitative analysis was evaluated in-depth with the aim of understanding which is the performance of each noise-reduction strategy. The results of this stage are summarized as follows:

- Visual inspection (qualitative analysis): the application of the SOR filter allow to remove a great part of the noise produced by the edge effect of the laser beam in all the combinations tested. This question is in line with the improvement with the results showed in Figure 3. Also, the application of the ANI and SBD improves the appearance of the results, offering sharper edges. In contrast to this, the application of the PCN algorithm (with and without SOR filtering) offers the worst results. This is because the presence of shrinkage effects.
- Bias results: in all the combination there is a bias error which could be attributed to the SLAM processing stage. This bias disappeared when the data is registered floor by floor, specially when the point cloud data is processing with the SOR filter.
- Dispersion results: the use of the standard deviation as well as the interpercentile values allow us to have an idea about the dispersion of the discrepancies. According to this, the use of the ANI or the SBD algorithms offer a general improvement of this aspect (Table 2 and Table 3). However, the use of the PCN algorithm does not improve the default results, especially due to the presence of shrinkage problems after several iterations.

3.4 Uncertainty propagation

The last stage of the study was to evaluate the effect of the discrepancies in the estimation of deflection in timber floors. To this end we have understand the discrepancies maps as a compound error (error in *x,y,z)*. So, the measure between points implies the introduction of this type of error two times.
According to this, the uncertainty propagation was performed by using the Monte Carlo approach with a total of 10.000 simulations. This approach was applied several times in accordance with the following inputs:

- Beam length: we have considered the most common values which are: 3.00/5.00/8.00 meters (Argüelles et al., 2013).
- Relative deflection: instead of using the deflection as input we propose the use of the relative deflection with the aim of clustering in different levels the uncertainty analysis. In this case we use four values for the relative deflection: L/300, L/200, L/100, L/50. The first value is the reference one in case of having partitions that could be affected by the deformation of the floor. The second one is a threshold commonly used due to the high stiffness of timber solutions (Argüelles et al., 2013). The rest are values which implies large deformations.

The moments (mean and standard deviation) of each input variable were modelled in accordance with the values of Table 2 and Table 3. For simplicity we have evaluated only the DEFAULT + SOR, ANI + SOR and SCB + SOR combinations. Both methods ANI+SOR and SBD + SOR proved to be efficient in the reduction of noise as it was showed in Table 1.
The results of the MonteCarlo simulations are showed in the following tables (Table 4, Table 5 and Table 6).

Beam length	Relative deflection	MonteCarlo (10.000 simulations)	
		Mean	Std.
3.00 m	L/300 (10 mm)	-	-
3.00 m	L/200 (15 mm)	-	-
3.00 m	L/100 (30 mm)	106	71
3.00 m	L/50 (60 mm)	51	6
5.00 m	L/300 (17 mm)	-	-
5.00 m	L/200 (25 mm)	218	96
5.00 m	L/100 (50 mm)	102	14
5.00 m	L/50 (100 mm)	50	3
8.00 m	L/300 (27 mm)	317	108
8.00 m	L/200 (40 mm)	206	37
8.00 m	L/100 (80 mm)	101	8
8.00 m	L/50 (160 mm)	50	2

Table 4. Results of the MonteCarlo simulation in case of considering the combination of DEFAULT + SOR

Beam length	Relative deflection	MonteCarlo (10.000 simulations)	
		Mean	Std.
3.00 m	L/300 (10 mm)	-	-
3.00 m	L/200 (15 mm)	220	159
3.00 m	L/100 (30 mm)	101	14
3.00 m	L/50 (60 mm)	50	3
5.00 m	L/300 (17 mm)	314	106
5.00 m	L/200 (25 mm)	206	36
5.00 m	L/100 (50 mm)	100	8
5.00 m	L/50 (100 mm)	50	2
8.00 m	L/300 (27 mm)	303	49
8.00 m	L/200 (40 mm)	202	21
8.00 m	L/100 (80 mm)	100	5
8.00 m	L/50 (160 mm)	50	1

Table 5. Results of the MonteCarlo simulation in case of considering the combination of ANI + SOR

Beam length	Relative deflection	MonteCarlo (10.000 simulations)	
		Mean	Std.
3.00 m	L/300 (10 mm)	-	-
3.00 m	L/200 (15 mm)	209	53
3.00 m	L/100 (30 mm)	101	10
3.00 m	L/50 (60 mm)	50	3
5.00 m	L/300 (17 mm)	304	61
5.00 m	L/200 (25 mm)	203	26
5.00 m	L/100 (50 mm)	100	6
5.00 m	L/50 (100 mm)	50	2
8.00 m	L/300 (27 mm)	300	35
8.00 m	L/200 (40 mm)	201	15
8.00 m	L/100 (80 mm)	100	4
8.00 m	L/50 (160 mm)	50	1

Table 6. Results of the MonteCarlo simulation in case of considering the combination of SBD + SOR

Additionally, we have calculated the relative deflection on 10 random beams of the timber floors of the study case (Figure 2). This stage was performed by a user expert in timber structures but not in 3D point clouds. The following table shows the results obtained during this stage (Table 7).

Combination	Length	Deflection	Ratio (Length/ Deflection)
DEFAULT + SOR (TLS)	4.252 (4.256)	0.058 (0.052)	73 (81)
	4.134 (4.159)	0.042 (0.051)	99 (82)
	3.857 (3.853)	0.064 (0.058)	60 (66)
	4.214 (4.199)	0.088 (0.071)	48 (59)
	4.224 (4.235)	0.072 (0.067)	59 (63)
	3.950 (3.952)	0.090 (0.084)	43 (46)
	3.872 (3.874)	0.089 (0.075)	43 (51)
	3.778 (3.759)	0.037 (0.023)	102 (163)
	3.047 (3.046)	0.028 (0.022)	109 (139)
	4.155 (4.175)	0.050 (0.064)	83 (65)
ANI +SOR (TLS)	4.247 (4.256)	0.058 (0.052)	73 (81)
	4.146 (4.159)	0.050 (0.051)	83 (82)
	3.849 (3.853)	0.061 (0.058)	63 (66)
	4.188 (4.199)	0.064 (0.071)	65 (59)
	4.213 (4.235)	0.060 (0.067)	70 (63)
	3.965 (3.952)	0.080 (0.084)	50 (46)
	3.872 (3.874)	0.070 (0.075)	55 (51)
	3.755 (3.759)	0.028 (0.023)	134 (163)
	3.044 (3.046)	0.025 (0.022)	123 (139)
	4.179 (4.175)	0.054 (0.064)	77 (65)
SBD + SOR (TLS)	4.250 (4.256)	0.054 (0.052)	79 (81)
	4.151 (4.159)	0.043 (0.051)	96 (82)
	3.847	0.060	64

	(3.853)	(0.058)	(66)
	4.196 (4.199)	0.066 (0.071)	63 (59)
	4.207 (4.235)	0.062 (0.067)	68 (63)
	3.948 (3.952)	0.083 (0.084)	47 (46)
	3.868 (3.874)	0.080 (0.075)	48 (51)
	3.761 (3.759)	0.027 (0.023)	140 (163)
	3.041 (3.046)	0.020 (0.022)	152 (139)
	4.166 (4.175)	0.064 (0.064)	65 (65)

Table 7. Results obtained during the extraction of measures from the different slabs

It is worth mentioning that the user found some problems during the analysis of the timber deflection in case of using the DEFAULT + SOR point cloud due to the dispersion of the data (**Figure 6**), requiring the support of an expert in 3D point cloud.

3.4.1 Discussion of the results obtained during the analysis of uncertainties: All the data generated during this stage was compared between them with the aim of analyzing the potential of the WMMS solution for diagnosis purposes. The results of this stage are summarized as follows:

- In all the cases (Monte Carlo simulation and manual deflection extraction) the combination of SBD + SOR shows the best results, followed by the ANI + SOR. This combination is able to improve from a deviation of 6 mm to 3 mm (100% of improvement), reducing the uncertainty when the user calculates the relative deflection.
- The WMMS point cloud, even if is processed with noise reduction algorithms, is not appropriated for a relative deflection of L/300. This question is also applicable for floors with a length of 3.00 m and a relative deflection of L/200. In all these cases the uncertainty is important.
- In case of inspecting floors with 5.00 m of span, the WMMS point cloud offers possibilities from L/200 to L/50 deflections. The best results are obtained when we use the SBR + SOR combination.
- For floors with 8.00 m of span the suitability of the system seem to be appropriated for the same range of relative deflections (L/200 to L/50). It is possible to apply the system for L/300 but with a high uncertainty (the standard deviation is the 10%).
- The uncertainties obtained during the MonteCarlo simulations are in line with those obtained by the expert user (manual analysis of deflections). In this case we have evaluated two floors with a length of about 3.5 meters and a relative deflection comprised between 150 and 50. The best performance was obtained by the combination of SBR + SOR with a mean discrepancy of 6.7 in comparison with the relative deflection obtained by the laser scanner. This discrepancy has a value of 9 in case of using the ANI + SOR filter and a value of 17 in case of using the DEFAULT + SOR combination.

4. CONCLUSIONS

This works aims at evaluating the possibility of using the WMMS point cloud as a source of information for performing deflection analysis in timber floors. According to this, we have tested different noise reduction strategies with the aim of improving the accuracy of the 3D point cloud. In this context several conclusions could be drawn:

- The edge effects that appears during the digitalization of timber floors could be mitigated by using a SOR filter. However, it is required to tune property these parameters since this filter could remove areas of interest.
- The Anisotropic filter proves to be an efficient filter for reducing part of the noise that appears in this type of sensors as well as improving the visual quality of the 3D point cloud. These effects are higher if a SOR filter is applied in combination with the Anisotropic one.
- Within the context of the Deep-Learning we have tested the PointCleanNet and the Score-based methods. The first one, which is based in the well-known architecture PointCleanNet, does not improve the quality of the WMMS point cloud. It is worth mentioning the presence of shrinkage. In contrast to this, the Score-based architecture proves to be efficient, improving the 3D point cloud from a qualitative and quantitative point of view.
- The uncertainties of the WMMS point cloud seems to be not appropriated for all the type of timber floors. According with our studies, this point cloud could be used in floors with a span of 5-8 meters and a relative deformation higher than L/200. In this case it is required the application of a noise-reduction strategy (ANI + SOR or SBD + SOR) to reduce the amount of dispersion of the data.
- The suggestion previous showed, which is based on a Monte Carlo simulation, proves to be in line with the results obtained in a real application.

Future works will be focused on applying the noise reduction strategy (ANI + SOR or SBD + SOR) over the entire point cloud. Then, we have planned to segment the 3D point cloud with the aim of locating the timber floors. This stage will be performed by using an Artificial Intelligence approach based on Machine/Deep Learning architectures. The application of both methods will allow to improve the inspection of historic timber floors. Additionally, we have planned to train all the Deep Learning architectures with data captured in other building (including TLS data that will act as ground truth).

ACKNOWLEDGEMENTS

This work has been supported by the Community of Madrid and the Higher Polytechnic School of Madrid through the Project CAREEN (desarrollo de nuevos métodos basados en inteligenCia ARtificial para la caracterización de daños en cosntruccioEs históricas a través de nubEs de puNtos 3D) with reference APOYO-JOVENES-21-RCDT1L-85-SL9E1R. This work has been also partially funded by the Spanish Ministry of Science and Innovation through the grant CAS21/00557. Finally, the authors would like to express their gratitude to the Department of Architectural Construction and Technology of the ETS of Architecture of the Universidad Politécnica de Madrid.

REFERENCES

Argüelles, R., Arriaga, F., Esteban, M., Iñiguez, G., Argüelles, R., 2013. Estructuras de madera. Bases de cálculo. AITIM, Madrid.

Besl, P.J., McKay, N.D., 1992. Method for registration of 3-D shapes. Presented at the Sensor fusion IV: control paradigms and data structures, Spie, pp. 586–606.

Camiña, J., Sánchez-Aparicio, L.J., Corrochano, C.M., Sanz-Arauz, D., González-Aguilera, D., 2022. Analysis of a SLAM-Based Laser Scanner for the 3D Digitalization of Underground Heritage Structures. A Case Study in the Wineries of Baltanas (Palencia, Spain). Presented at the The Future of Heritage Science and Technologies: ICT and Digital Heritage: Third International Conference, Florence Heri-Tech 2022, Florence, Italy, May 16–18, 2022, Proceedings, Springer, pp. 42–56.

Di Filippo, A., Sánchez-Aparicio, L.J., Barba, S., Martín-Jiménez, J.A., Mora, R., González Aguilera, D., 2018. Use of a wearable mobile laser system in seamless indoor 3D mapping of a complex historical site. Remote Sensing 10, 1897.

Garcia-Martin, R., López-Rebollo, J., Sánchez-Aparicio, L.J., Fueyo, J.G., Pisonero, J., Gonzalez-Aguilera, D., 2020. Digital image correlation and reliability-based methods for the design and repair of pressure pipes through composite solutions. Construction and Building Materials 248, 118625.

Girardeau-Montaut, D., Roux, M., Marc, R., Thibault, G., 2005. CHANGE DETECTION ON POINTS CLOUD DATA ACQUIRED WITH A GROUND LASER SCANNER.

Lague, D., Brodu, N., Leroux, J., 2013. Accurate 3D comparison of complex topography with terrestrial laser scanner: Application to the Rangitikei canyon (N-Z). ISPRS Journal of Photogrammetry and Remote Sensing 82, 10–26. https://doi.org/10.1016/J.ISPRSJPRS.2013.04.009

Luo, S., Hu, W., 2021. Score-based point cloud denoising. Presented at the Proceedings of the IEEE/CVF International Conference on Computer Vision, pp. 4583–4592.

Marelli, S., Sudret, B., 2014. UQLab: A framework for uncertainty quantification in Matlab, in: Vulnerability, Uncertainty, and Risk: Quantification, Mitigation, and Management. pp. 2554–2563.

Nocerino, E., Menna, F., Remondino, F., Toschi, I., Rodríguez-Gonzálvez, P., 2017. Investigation of indoor and outdoor performance of two portable mobile mapping systems, in: Remondino, F., Shortis, M.R. (Eds.), . Presented at the SPIE Optical Metrology, Munich, Germany, p. 103320I. https://doi.org/10.1117/12.2270761

Nocerino, E., Rodríguez-Gonzálvez, P., Menna, F., 2019. Introduction to mobile mapping with portable systems, in: Laser Scanning. CRC Press, pp. 37–52.

Qi, C.R., Su, H., Mo, K., Guibas, L.J., 2017. Pointnet: Deep learning on point sets for 3d classification and segmentation. Presented at the Proceedings of the IEEE conference on computer vision and pattern recognition, pp. 652–660.

Rakotosaona, M., La Barbera, V., Guerrero, P., Mitra, N.J., Ovsjanikov, M., 2020. Pointcleannet: Learning to denoise and remove outliers from dense point clouds. Presented at the Computer graphics forum, Wiley Online Library, pp. 185–203.

Rodríguez-Gonzálvez, P., Jimenez Fernandez-Palacios, B., Muñoz-Nieto, Á.L., Arias-Sanchez, P., Gonzalez-Aguilera, D., 2017. Mobile LiDAR system: New possibilities for the documentation and dissemination of large cultural heritage sites. Remote Sensing 9, 189.

Rodríguez-Martín, M., Rodríguez-Gonzálvez, P., González-Aguilera, D., Nocerino, E., 2018. Novel Approach for Three-Dimensional Integral Documentation of Machine Rooms in Hospitals Using Portable Mobile Mapping System. IEEE Access 6, 79200–79210. https://doi.org/10.1109/ACCESS.2018.2884922

Rusu, R.B., Cousins, S., 2011. 3d is here: Point cloud library (pcl). Presented at the 2011 IEEE international conference on robotics and automation, IEEE, pp. 1–4.

Sánchez-Aparicio, L.J., Conde, B., Maté-González, M.A., Mora, R., Sánchez-Aparicio, M., García-Álvarez, J., González-Aguilera, D., 2019. A COMPARATIVE STUDY between WMMS and TLS for the STABILITY ANALYSIS of the SAN PEDRO CHURCH BARREL VAULT by MEANS of the FINITE ELEMENT METHOD, in: International Archives of the Photogrammetry, Remote Sensing and Spatial Information Sciences - ISPRS Archives. International Society for Photogrammetry and Remote Sensing, pp. 1047–1054. https://doi.org/10.5194/isprs-archives-XLII-2-W15-1047-2019

Sánchez-Aparicio, L.J., Mora, R., Conde, B., Maté-González, M.Á., Sánchez-Aparicio, M., González-Aguilera, D., 2021. Integration of a wearable mobile mapping solution and advance numerical simulations for the structural analysis of historical constructions: A case of study in San Pedro Church (Palencia, Spain). Remote Sensing 13, 1252.

Villanueva Llauradó, P., Maté González, M.A., Sánchez-Aparicio, L.J., Benito Pradillo, M.Á., González-Aguilera, D., García Palomo, L.C., 2022. A comparative study between a static and a mobile laser scanner for the digitalization of inner spaces in historical constructions. Rehabend.

Xu, Z., Foi, A., 2019. Anisotropic denoising of 3D point clouds by aggregation of multiple surface-adaptive estimates. IEEE Transactions on Visualization and Computer Graphics 27, 2851–2868.

Yang, S., Xu, S., Huang, W., 2022. 3D Point Cloud for Cultural Heritage: A Scientometric Survey. Remote Sensing 14, 5542. https://doi.org/10.3390/rs14215542

Zhang, J., 2021. Modern Monte Carlo methods for efficient uncertainty quantification and propagation: A survey. Wiley Interdisciplinary Reviews: Computational Statistics 13, e1539.